# The deep spectrophotometric mosaic of the Orion Nebula. Preliminary results

**M. Núñez-Díaz**[1,2]**, C. Esteban**[1,2]**, and A. Mesa-Delgado**[1,2,3]

[1] Instituto de Astrofísica de Canarias, E-38200 La Laguna, Tenerife, Spain
[2] Departamento de Astrofísica, Universidad de La Laguna, E-38205 La Laguna, Tenerife, Spain
[3] Departamento de Astronomía y Astrofísica, Facultad de Física, Pontificia Universidad Católica de Chile, Av. Vicuña Mackenna 4860, 782-0436 Macul, Santiago, Chile

## Abstract

We present a deep spectrophotometric mosaic of the Orion Nebula obtained with the Potsdam Multi-Aperture Spectrophotometer (PMAS) at Calar Alto Observatory. The aim of the observations has been to determine the spatial distribution of physical conditions and chemical abundances across the nebula and at different morphological structures. The 64 arcsec long hexagonal fiber bundle (PPAK) has been used to obtain a complete mosaic of the central 4 arcmin of the nebula in about 16 fields. The spectra cover the whole optical spectral range and permits to derive: a) different line intensity ratios covering all possible ionization states in the nebula; b) electron densities diagnostics based of [S II], [O II], [Cl III] and [Fe III] line ratios; c) electron temperatures from [O III], [N II] and [S II] line ratios as well as the Balmer discontinuity; d) the distribution of ionic and total abundances determined from collisionaly excited lines; e) ionic abundances of $C^{2+}$ and $O^{2+}$ from recombination lines; f) and the abundance discrepancy factor for $O^{2+}$.

## 1 Introduction

H II regions are tracers of the chemical composition of the Universe from the local interstellar medium to the high-redshift starburst galaxies. We still naively tend to describe then as homogeneous spheres of ionized gas but reality is far more complicated. For example, recent results of our group for the Orion Nebula [3, 4, 5, 6, 7] show that small spatial scale variations of density and temperature are present and could be even very large in some cases and may affect the abundance determinations. An old controversy is still open about the presence of temperature fluctuations in ionized nebulae (the so-called $t^2$ parameter introduced by [8]).

If these fluctuations are real, the abundance data that we commonly use for many cosmic objects would be underestimated. Another unsolved problem in nebular physics is that ionic abundances determined from recombination lines (RLs) are always larger than those obtained from collisionally excited ones (CELs) of the same ion. This is the so-called *abundance discrepancy* problem (AD). [14] suggested that both, $t^2$ and AD are genetically related but others as [13] consider that the AD is produced by small spatial scale chemical inhomogeneities in the interstellar medium. Recently, [15] and [6] have claimed to have solved the AD problem in proplyds by subtracting the local nebula background and using correct values of electron density. [15] suggest that in the presence of a population of small and partially ionized clumps along a random line of sight, the CEL-derived Orion nebula gaseous abundances would be lower limits and therefore density inhomogeneities are playing havoc with the classic forbidden-line diagnostics. The immediate precedent of the present project is the work by [11] that show some results of a mosaic of the central 6 arcmin of the Orion Nebula taken with the same instrument. Although their exposures times were very much shorter (only 2s) and with lower spectral resolution.

## 2    Observations and data reduction

The observations were carried out at the 3.5m telescope of the Calar Alto observatory with the PMAS [10] in the PPAK mode [1] a fibre bundle IFU with an hexagonal FoV covering $72\times64$ arcsec$^2$ (65% of filling factor) and a diameter of 2.7 arcsec per fiber. The grating V1200 has been used with a spectral resolution of $\sim 2$ Å  FWHM, enough to separate the [O III] 4363 Å  line from telluric features to determine $T_e$([O III]) as well as to separate the brightest O II lines at 4650 Å from nearby [Fe III] lines. We have observed three different ranges, covering the whole optical range (see Table 1 for details). The initial pointing was centered on the Trapezium star $\theta^1$ Ori C and the rest has followed an hexagonal pattern adjusting them to the shape of the PPAK science bundle, having a common area at the edges of the hexagons of each pair of adjacent pointings. The total number of pointings has been 16 (except for the green spectral range) covering the inner 4 arcmin of the nebula, and taken in 3 different campaigns January 2010, November and December 2011. The data were reduced with the P3D software [12] developed by the PMAS team in Potsdam and IRAF for the flux calibration. Emission line fluxes were measured using our own IRAF scripts to automatize the process. The electron density was computed using the PyNeb tool [2].

Table 1: Observation layout

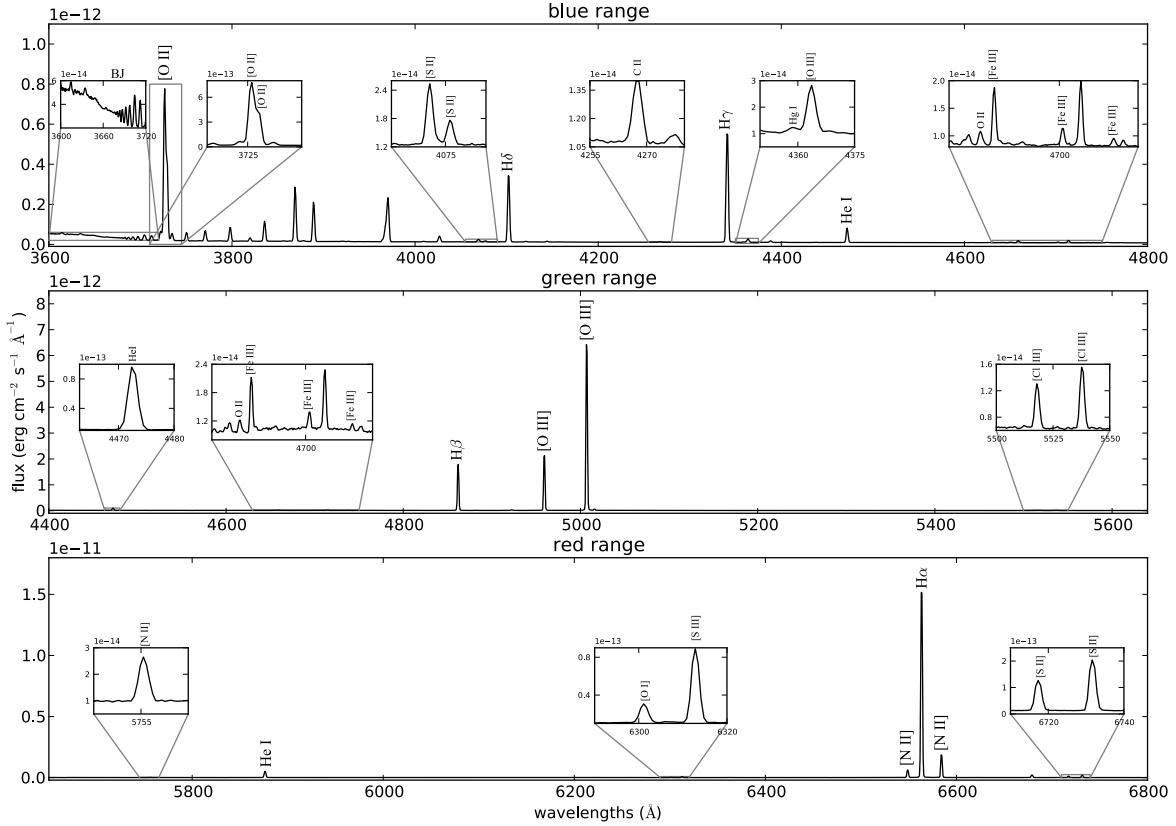| Range | $\Delta\lambda$ (Å) | exp. time long (s) | exp. time short (s) | No. pointings | No. spectra |
|---|---|---|---|---|---|
| blue | 3550-4800 | $3\times600$ | $3\times10$ | 16 | 5296 |
| green | 4400-5640 | $3\times90$ | $3\times10$ | 15 | 4965 |
| red | 5650-6800 | $3\times90$ | $3\times10$ | 16 | 5296 |

Figure 1:   The three spectral ranges observed showing several important emission lines and zooming-up the faint ones. The blue, green and red spectral range corresponds to the top, middle and bottom panel, respectively. The spectrum plotted corresponds to a single spaxel located at $\sim 42''$ northwest of the Trapezium.

# 3    Data description

In Fig. 1, we show the three spectral ranges and observed several important emission lines. The blue range has the longest exposure times, being able to measure the faint C II and O II RLs, and the Balmer discontinuity for at least half of the spaxels.  Also, the selected spectral resolution allows us to deblend [O II] 3726+3729 Å , [S II] 4068+4076 Å and Hg I 4358+[O III] 4363 Å. In addition to the bright lines (H$\beta$, [O III], He I), in the green range we also detect the faint [Cl III] doublet with good signal to noise ratio.  These two ranges share in common the He I 4471 Å line useful for re-scaling both spectral ranges. Finally, we measure the diagnostic lines of [N II] and [S II], plus the H$\alpha$ emission in the red spectral range.
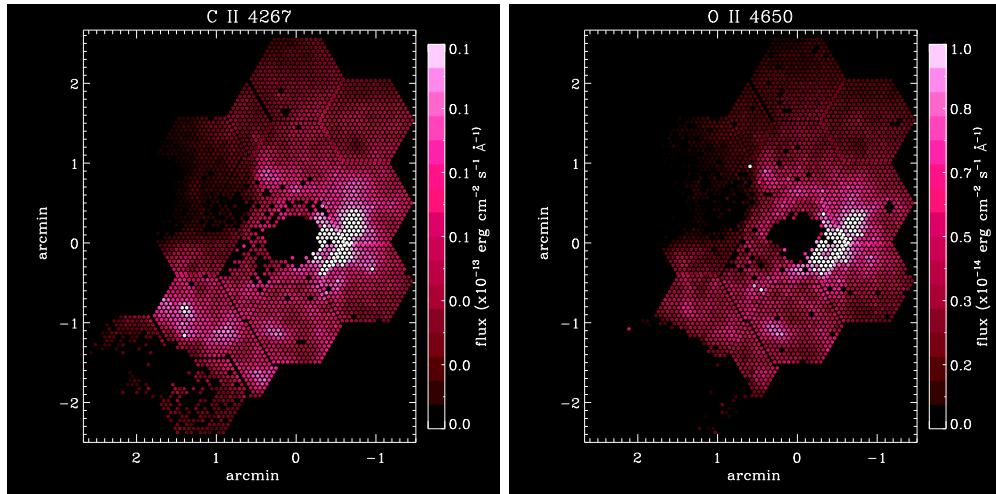
Figure 2: Spatial distribution of the faint RLs of C II 4267 Å (left) and O II 4650 Å (right).
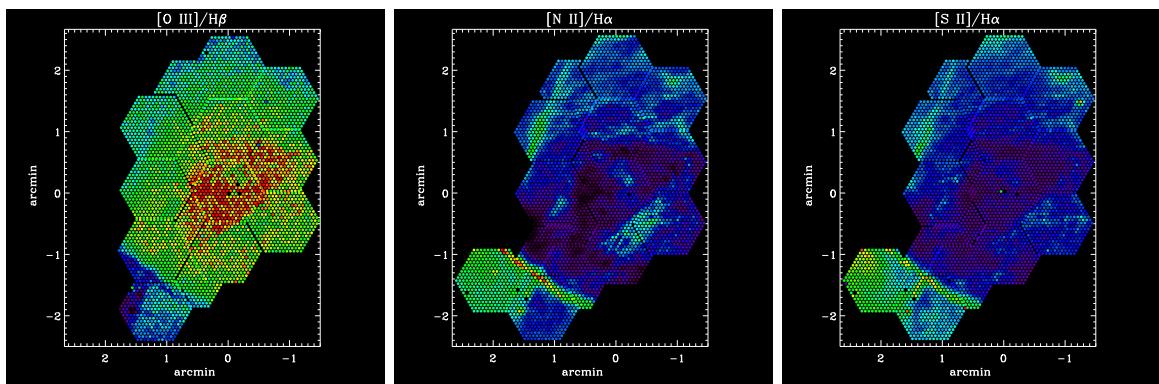


Figure 3: Ionization structure of the nebula. From left to right: [O III]/Hβ, [N II]/Hα and [S II]/Hα.

## 4  Preliminary results

### 4.1  Recombination lines

In Fig. 2 we show for the first time the spatial distribution of the faint RLs of C II (left panel) and O II (right panel). Both emission lines present the highest values at the west of the Trapezium stars and the lowest at the "Dark Bay" and outside of the Orion bar ionization front. The maxima of the O II emission line are somewhat inner than the C II, as expected from their ionization potentials. It is also remarkable the bright clumps closer to the Orion bar.
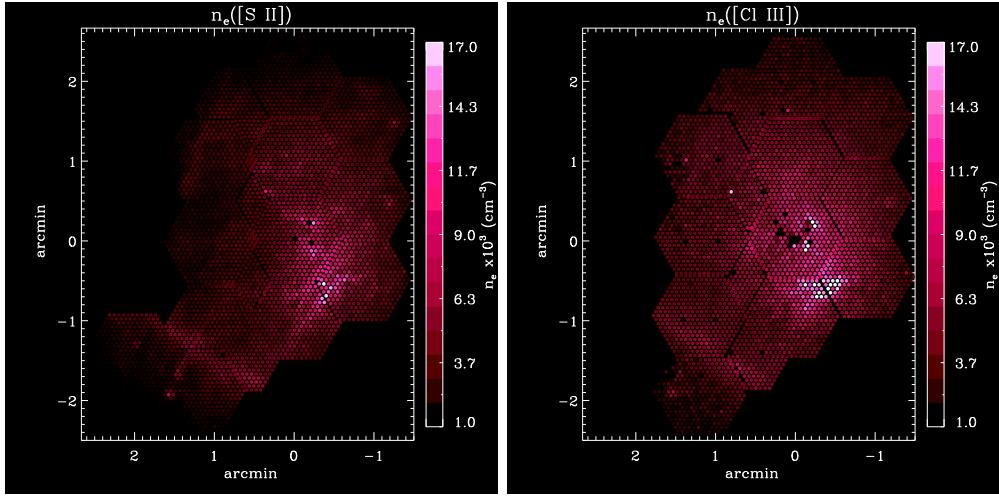
Figure 4:    Electron density distribution computed through two different diagnostic ratios and assuming a constant electron temperature of 10,000 K. On the left-hand side, $n_e$([S II]) and on the right-hand side $n_e$([Cl III]).

## 4.2    Ionization structure

The most immediate result is the ionization structure of the nebula, which can be investigated by exploring the line ratio maps of usual diagnostic lines. Fig. 3 shows the line ratio maps for [O III]/H$\beta$, [N II]/H$\alpha$ and [S II]/H$\alpha$. The [O III] emission is originated in the fully ionized zones at the center of the nebula, tracing the level of ionization in these zones, while [N II] and [S II] are originated in the single ionized regions between the ionized and partially ionized zones of the nebula. The Orion bar is the most prominent substructure, clearly seen as a diagonal region south-east of the Trapezium. The [O III]/H$\beta$ ratio decreases where [N II]/H$\alpha$ and [S II]/H$\alpha$ enhance, showing the effective reciprocity between them. As already noticed by [9], the [N II]/H$\alpha$ ratio is very rich in substructures.

## 4.3    Electron density

We computed the electron density using the [S II] 6716, 6731 Å and the [Cl III] 5517, 5537 Å ratios for the red and green ranges, respectively, and considering a constant electron temperature of 10,000 K. Fig. 4 shows the electron density maps of both diagnostics. In one hand, the highest densities are found in a region at the southwest of the Trapezium of the order of $1.5 \times 10^4$ cm$^{-3}$, clearly seen in the $n_e$([Cl III]) map. In the other hand, the lowest values are found in the Orion "Dark Bay" and the regions far away from the Trapezium. It also occurs local enhancement as for example the Orion bar ionization front, Herbig-Haro objects and proplyds, which are more clearly seen in the $n_e$([S II]) map.

# 5  Conclusions

Considering the aforementioned, these data are of unparalleled quality allowing us to measure the physical conditions of the nebula through four different diagnostics: lines ratios of [Cl III], [S II], [O II] and [Fe III ] for the e lectron density; [O III], [N II], [S II] line ratios and as well as the Balmer discontinuity for the electron temperature. We are also able to map for the first time in the Orion nebula the intensity distribution of C II and O II RLs . We can also determine spatial distribution of ionic and total abundances of several CELs and the RLs of C II and OII. Furthermore, we could calculate the abundance discrepancy factor of the $O^{2+}$ ion. The data gathered will permit to correlate the different known nebular structures at intermediate and large spatial scales and the derived physical conditions and other properties of the gas with an unprecedented signal-to-nosie ratio.

# References

[1]  Kelz, A., Verheijen, M.A.W., Roth, M.M., et al. 2006, PASP, 118, 129

[2]  Luridiana, V. and Morisset, C., & Shaw, R. A. 2012, IAU Symposium, 283, 422

[3]  Mesa-Delgado, A., Esteban, C., & García-Rojas, J. 2008, ApJ, 675, 389

[4]  Mesa-Delgado, A., López-Martín, L., Esteban, C., et al., 2009, MNRAS, 394, 693

[5]  Mesa-Delgado, A., Núñez-Díaz, M., Esteban, C., et al. 2011, MNRAS, 417, 420

[6]  Mesa-Delgado, A., Núñez-Díaz, M., Esteban, C., et al. 2012, MNRAS, 426, 614

[7]  Núñez-Díaz, M., Mesa-Delgado, A., Esteban, C., et al. 2012, MNRAS, 421, 3399

[8]  Peimbert, M. 1967, ApJ, 150, 825

[9]  Pogge, R. W., Owen, J. M., & Atwood, B. 1992, ApJ, 399, 147

[10]  Roth, M.M., Kelz, A., Fechner, T., et al. 2005, PASP, 117, 620

[11]  Sánchez, S. F., Cardiel, N., Verheijen, M. A. W., et al. 2007, A&A, 465, 207

[12]  Sandin, C., Becker, T., Roth, M. M., et al. 2010, A&A, 515, A35

[13]  Stasińska, G., Tenorio-Tagle, G., Rodríguez, M., & Henney, W. J. 2007, A&A, 471, 193

[14]  Torres-Peimbert, S., Peimbert, M., & Daltabuit, E. 1980, ApJ, 238, 133

[15]  Tsamis, Y. G., Walsh, J. R., Vílchez, & J. M. Péquignot, D. 2011, MNRAS, 412, 1367